Tunable surface plasmon polaritons in Ag composite films by adding dielectrics or semiconductors

Dylan Lu,[1] Jimmy Kan,[2] Eric E. Fullerton,[1,2] and Zhaowei Liu[1,a)]
[1]*Department of Electrical and Computer Engineering, University of California, San Diego, 9500 Gilman Drive, La Jolla, California 92093, USA*
[2]*Center for Magnetic Recording Research, University of California, San Diego, 9500 Gilman Drive, La Jolla, California 92093, USA*

(Received 28 April 2011; accepted 25 May 2011; published online 16 June 2011)

We demonstrate that the surface plasmon polariton (SPP) properties of the silver composite films can be tuned by modest additions of silicon oxide or silicon. The dispersion relations deviate from that of pure silver films, and exhibit the capability to shift the surface plasmon frequency and provide larger SPP wave vectors at longer wavelengths. The effective permittivities are modeled phenomenologically by taking into account both filling ratios and size effects. These types of tunable composite films have various useful applications in areas, such as superlens imaging, SPP based sensing, enhanced photoluminescence, and SPP based photovoltatics. © *2011 American Institute of Physics*. [doi:10.1063/1.3600661]

Recent studies on the fundamental properties of surface plasmon polaritons (SPPs) have provided better understanding of physical phenomena in the field of plasmonic science and have inspired exciting applications of SPP based structures and devices.[1–3] SPPs are quasiparticles excited at metal–insulator interfaces through resonant coupling of electromagnetic (EM) waves to the free electrons in the metal.[4] The dispersion curve of SPP lies below the light line in the corresponding surrounding medium, resulting in a concentration of EM energy into the subwavelength scale.[5] Due to the reduced length scales and quick response speed of SPPs, applications include light guiding and manipulation at the nanoscale,[6,7] subdiffraction-limited optical imaging,[8,9] highly sensitive detection,[10] ultrafast optoelectronic devices,[11,12] highly efficient light emission,[13] and enhanced solar energy efficiency.[14] All these applications rely on the unique wavelength-dependent SPP mode properties and the dispersive permittivity profiles associated with a set of existing materials, which limits the applicability of SPP technologies.

To address this limitation of material properties, artificially nanostructured materials often exhibit extraordinary properties not found in nature.[15,16] Theoretical descriptions and experimental results detailing the optical properties of metal clusters have been extensively discussed as a pathway to modify material properties.[15] Recent investigations on silver-gold clusters reveal that their plasmonic band evolves with the particle size and relative concentrations, which are well predicted by a model based on the time-dependent local-density approximation.[17] The tunability of metal alloys has been utilized to optimize the enhanced emission from semiconductors.[18] Metals mixed with dielectrics provide an alternative route toward engineered SPP properties.[19] It has been proposed that a composite metal-dielectric films enables superlenses working at any desired wavelength with a designed metal filling factor.[20] Efforts have been made to fabricate smooth metal-dielectric nanocomposite films but their absorption spectra and retrieved material properties do not agree well with effective medium theory.[21,22]

In this letter, we describe modifying the optical properties of metals by adding a small percentage of dielectrics or semiconductors. We have studied Ag films mixed with SiO_2 or Si where the SPPs are excited and measured. Angular-resolved reflection spectra at different wavelengths are obtained in the Fourier space and agreed well with a theoretical model. Effective material properties of such composite films are also derived and discussed.

The optical properties of composite films can be characterized by measuring their angular-resolved reflection spectra at different wavelengths using an oil-immersion optical microscope as illustrated in Fig. 1. The numerical aperture (NA) of the oil immersion objective is NA=1.4. Monochromatic waves produced by passing a broadband light source through a series of bandpass optical filters are incident onto the composite film samples from the glass substrate side. A charge coupled device (CCD) camera located at the back-focal plane of the objective lens captures the reflection in the Fourier space. At a certain wave vector, phase matching con-

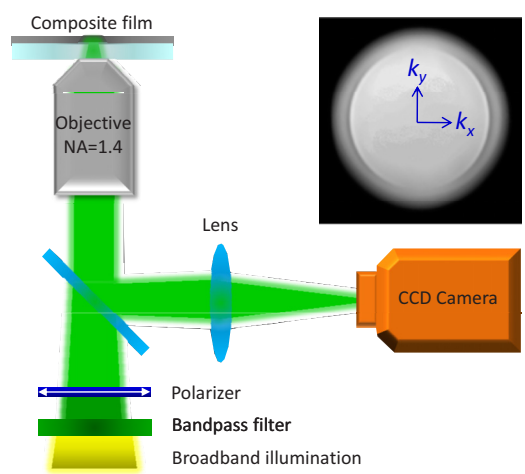

FIG. 1. (Color online) Schematic configuration of an oil-immersion optical microscope system for characterizing the SPP properties of composite films at different wavelengths. The inset picture gives a typical reflection at the back-focal plane of the system captured by a CCD camera.

a)Author to whom correspondence should be addressed. Electronic mail: zhaowei@ece.ucsd.edu.

 © 2011 American Institute of Physics

Author complimentary copy. Redistribution subject to AIP license or copyright, see http://apl.aip.org/apl/copyright.jsp

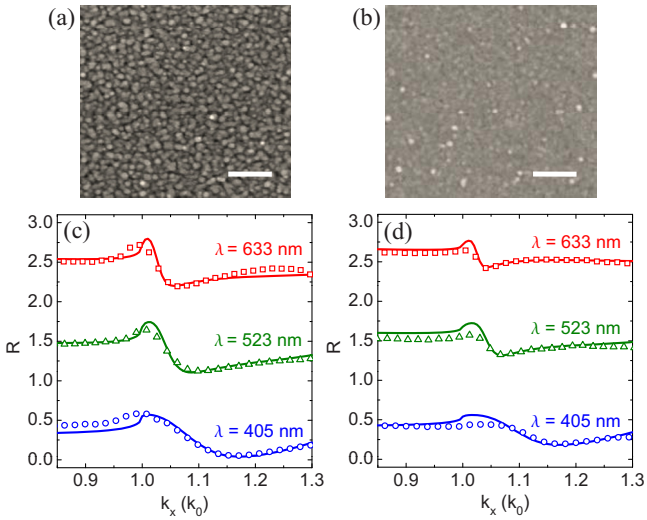

FIG. 2. (Color online) SEM images for the fabricated composite films: (a) Ag–SiO_2 composite film of 30 nm thick with 4.7% atom SiO_2; (b) Ag–Si composite film of 40 nm thick with 5% atom Si; with the scale bar to be 100 nm. Measured angular-resolved reflection spectra (open circles, open triangles, and open squares) and theoretical fit curves (solid lines) for (c) Ag–SiO_2; and (d) Ag–Si at the wavelengths λ=405 nm, 523 nm, and 633 nm, respectively.

ditions are satisfied to excite SPPs at the film–air interface by the P-polarized light. This excitation is visualized as a dip in the captured reflection intensity. A linear polarizer is used to filter out the S-polarized component.

The composite films were fabricated by doping a small amount of SiO_2 or Si into pure silver. The Ag–SiO_2 (30 nm thick with 4.7% atom SiO_2) and Ag–Si (40 nm thick with 5% atom Si) composite films were prepared by cosputtering onto ambient temperature glass substrates from magnetron sputtering sources. Corresponding scanning electron microscope (SEM) images are given in Figs. 2(a) and 2(b), respectively. Sputtering rates for dc-sputtered Ag and Si at 50 W were 1.6 Å/s and 0.16 Å/s, respectively. SiO_2 was rf sputtered at 90 W at a rate of 0.17 Å/s. The sputtering rates were determined by low angle x-ray reflectivity measurements of total film thicknesses versus time. The base pressure of the chamber was $5-8\times10^{-9}$ Torr and the Ar pressure during sputtering was fixed at 2.5 mTorr. Average compositions are determined stoichiometrically based on material deposition rates.

The inset in Fig. 1 gives a typical reflection intensity profile at the back-focal plane of the microscope (this case λ=523 nm). The radius of the reflected intensity disk is limited by the NA of the oil-immersion objective corresponding to a free-space wave vector, i.e., $NA=1.4k_0$, while the symmetric dark rings inside the bright disk indicates the position of the SPP excitation in the k space. The reflection images at the Fourier plane for different wavelengths across the optical spectrum are taken for both Ag–SiO_2 and Ag-Si composite films. After normalized by the corresponding incident light intensity, the reflection spectra are retrieved along the k_x axis for each wavelength. Three experimental curves for the wavelengths λ=405, 523, and 633 nm obtained following this method are plotted as open symbols in Figs. 2(c) and 2(d) for Ag–SiO_2 and Ag–Si composite films, respectively. The intensity peak around k_0 in each curve corresponds to where total internal reflection takes place while the intensity dip afterwards indicates the excitation of SPPs when the parallel wave vector k_x matches the wave vector of SPP resonances at the film–air interface. Similar to those in pure metals, the SPPs in the composite films shift to higher wave vectors with broadened resonance bandwidths when the incident wavelength blueshifts.

To get a better understanding of the effective material properties of the metal film after being doped with a small percentage of dielectrics or semiconductors, a simple phenomenological model was investigated to fit the experimental results. The effective dielectric function of the metal-dielectric composites was assumed to follow the Maxwell–Garnett formalism or the Bruggerman mixing theory.[20] In the case of a small fraction of dielectrics, the percolation of metal dominates the optical properties of the composite films. Therefore, we approximate the effective dielectric function $\varepsilon_{eff}(\omega,x)$ for the composite film $Ag_{(1-x)}D_x$ as the volumetric average of the metal Ag and the doping D components as follows:[17,23]

$$\varepsilon_{eff}(\omega,x) = \varepsilon_{Ag}(\omega)(1-x') + \varepsilon_D(\omega)x', \quad (1)$$

where D stands for the doped dielectric or semiconductors, whose volume percentage x' can be calculated from its mole fraction x in the composite film as $x'=xV_D/[xV_D+(1-x)V_{Ag}]$ with V as the volume per mole. The permittivity $\varepsilon_D(\omega)$ for SiO_2 and Si are taken from Refs. 24 and 25, respectively. The Drude model is used to characterize the metal Ag in the optical spectral range; $\varepsilon_{Ag}(\omega)=\varepsilon_\infty-\omega_p^2/(\omega^2-i\gamma'\omega)$, where for Ag, the high-frequency permittivity $\varepsilon_\infty=6.0$, the plasma frequency $\omega_p=1.5\times10^{16}$ rad/s obtained by fitting the model to the experimental data taken from Ref. 26, and γ' is the relaxation frequency.

In contrast with the pure metal film, the optical properties of the composite film depend strongly on the details of the nanostructures, especially the critical length scales of the heterogeneities.[17] The relaxation frequency γ' is no longer a constant but depends on the particle or grain size and doped media,[22,27,28]

$$\gamma' = \gamma + A\frac{v_F}{R}, \quad (2)$$

where $\gamma=7.73\times10^{13}$ rad/s is the relaxation frequency for bulk Ag when fitted to the experimental data in Ref. 26, $v_F=1.39\times10^6$ m/s is the Fermi velocity. R corresponds to the averaged particle or grain radius obtained from SEM pictures in Figs. 2(a) and 2(b) as $R=10$ nm and 5 nm for Ag–SiO_2 and Ag–Si composite films, respectively. The characteristic parameter A includes both the quantum size effect in extremely small particles of free surface and the dynamic interface charge transition effect between Ag particles and the embedded dopant,[27] and therefore is used as the only fit parameter in this model to capture the resonance positions and bandwidths of SPPs.

With the effective dielectric functions for the composite films assigned, the multilayer system in the simulation is a composite film sandwiched between two infinite dielectric claddings, glass ($n=1.5$) and air ($n=1.0$). The thickness of the composite film is set according to the fabricated samples (30 nm for Ag–SiO_2 and 40 nm for Ag–Si). Reflection spectra for different wavelengths at the glass side are calculated using a transfer matrix method.[29] The simulated reflection curves are plotted as solid lines alongside the experimental data in Figs. 2(c) and 2(d). The simulations reproduce the key features of the experimental data, accurately depicting

Author complimentary copy. Redistribution subject to AIP license or copyright, see http://apl.aip.org/apl/copyright.jsp

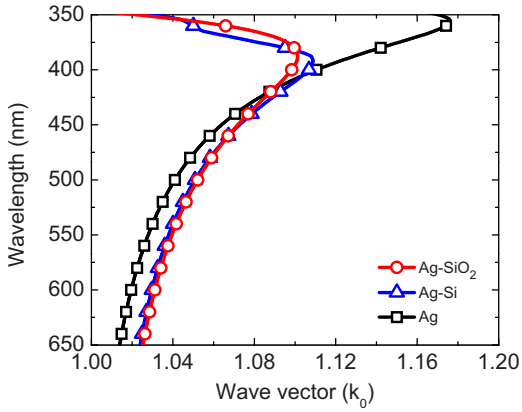

FIG. 3. (Color online) SPP dispersion relations for Ag–SiO_2 (red line with open circles) and Ag–Si (blue line with open triangles) composite films. Pure Ag film is present in black line with open squares as a comparison.

the approximate positions of total internal reflection peaks and SPP resonances. The fit parameter $A=1.5$ and 0.6 are used for Ag–SiO_2 [Fig. 2(c)] and Ag-Si [Fig. 2(d)] composite films, respectively. Therefore the relaxation frequency γ' for Ag mixed with a small amount of SiO_2 and Si are found to be 138.73×10^{13} rad/s and 112.53×10^{13} rad/s, respectively, which are about one order of magnitude larger than that for bulk Ag. It thereby indicates a stronger scattering loss in the composite films. By using the modified relaxation frequency, this theoretical model well characterizes the SPP resonances at different wavelengths for both doped samples.

The SPP dispersion relation at the film–air interface can be obtained from the effective dielectric function of the composite film by $k_x=k_0\sqrt{\varepsilon_{\mathrm{air}}\varepsilon_{\mathrm{eff}}(\omega)/[\varepsilon_{\mathrm{air}}+\varepsilon_{\mathrm{eff}}(\omega)]}$. As a comparison, the permittivity for a pure Ag film is also retrieved following the same method. Figure 3 shows the dispersion relation for the fabricated Ag–SiO_2 (in red) and Ag–Si (in blue) composite films as well as for the Ag film (in black). The SPP dispersion of Ag film after being doped with a small amount of SiO_2 or Si deviates from that of a pure Ag film. For Ag–SiO_2 composite films, the surface plasmon frequency redshifts to $\lambda_{SP}\sim385$ nm from originally $\lambda_{SP}\sim355$ nm while for Ag–Si composite films, it goes even further to $\lambda_{SP}\sim400$ nm. In principle, larger-percent dopants will enable even larger shifts toward possibly green wavelengths. This designable SPP property opens up the possibility of applications at different wavelengths. In addition, at wavelengths longer than 425 nm, the composite films have the advantage to provide larger SPP wave vectors than the pure metal film, and therefore a higher EM field confinement is expected.

In the composite film fabrication, the film thickness has been optimized to provide a pronounced measurement. Highly doped composite films produce unidentifiable wide resonances. Losses in such highly doped composite films become pronounced, leading to very wide bandwidths and less conspicuous resonance dips. A potential solution for more flexible tunability of the SPP dispersion in composite films is to investigate binary or ternary alloy systems, such as Ag–Au or Ag–Al.

In conclusion, by charactering the optical properties of composite films, we demonstrate a promising way to tune the SPP properties of existing metal films by adding additional dielectrics or semiconductors. A phenomenological model that takes into account the filling ratio and particle size effect describes the effective material properties of the measured composite films, and shows their distinct difference from pure metal films. The ability to tune these material properties opens the door toward various useful applications, such as superlens imaging, SPP based sensors, enhanced photoluminescence, and SPP based photovoltatics, etc.

This work is partially supported by the startup fund of the University of California at San Diego and the NSF-ECCS under Grant No. 0969405.

[1]H. R. Raether, *Surface Plasmons on Smooth and Rough Surfaces and on Gratings* (Springer, New York, 1988).
[2]M. L. Brongersma and P. G. Kik, *Surface Plasmon Nanophotonics* (Springer, Dordrecht, 2007).
[3]J. A. Schuller, E. S. Barnard, W. Cai, Y. C. Jun, J. S. White, and M. L. Brongersma, Nature Mater. **9**, 193 (2010).
[4]S. A. Maier, *Plasmonics: Fundamentals and Applications* (Springer Science+Business Media, New York, 2007).
[5]W. L. Barnes, A. Dereux, and T. W. Ebbesen, Nature (London) **424**, 824 (2003).
[6]T. W. Ebbesen, H. J. Lezec, H. F. Ghaemi, T. Thio, and P. A. Wolff, Nature (London) **391**, 667 (1998).
[7]S. A. Maier, P. G. Kik, H. A. Atwater, S. Meltzer, E. Harel, B. E. Koel, and A. A. G. Requicha, Nature Mater. **2**, 229 (2003).
[8]N. Fang, H. Lee, C. Sun, and X. Zhang, Science **308**, 534 (2005).
[9]Z. Liu, H. Lee, Y. Xiong, C. Sun, and X. Zhang, Science **315**, 1686 (2007).
[10]G. Konstantatos and E. H. Sargent, Nat. Nanotechnol. **5**, 391 (2010).
[11]E. Ozbay, Science **311**, 189 (2006).
[12]K. F. MacDonald, Z. L. Sámson, M. I. Stockman, and N. I. Zheludev, Nat. Photonics **3**, 55 (2009).
[13]K. Okamoto, I. Niki, A. Shvartser, Y. Narukawa, T. Mukai, and A. Scherer, Nature Mater. **3**, 601 (2004).
[14]H. A. Atwater and A. Polman, Nature Mater. **9**, 205 (2010).
[15]U. Kreibig and M. Vollmer, *Optical Properties of Metal Clusters* (Springer, New York, 1995).
[16]V. M. Shalaev, Nat. Photonics **1**, 41 (2007).
[17]M. Gaudry J. Lermé, E. Cottancin, M. Pellarin, J. L. Vialle, M. Broyer, B. Prével, M. Treilleux, and P. linon, Phys. Rev. B **64**, 085407 (2001).
[18]D. Y. Lei, J. Li, and H. C. Ong, Appl. Phys. Lett. **91**, 021112 (2007).
[19]V. M. Shalaev, *Nonlinear Optics of Random Media: Fractal Composites and Metal-Dielectric Films* (Springer, New York, 2000).
[20]W. Cai, D. A. Genov, and V. M. Shalaev, Phys. Rev. B **72**, 193101 (2005).
[21]R. B. Nielsen, M. D. Thoreson, W. Chen, A. Kristensen, J. M. Hvam, V. M. Shalaev, and A. Boltasseva, Appl. Phys. B: Lasers Opt. **100**, 93 (2010).
[22]W. Chen, M. D. Thoreson, A. V. Kildishev, and V. M. Shalaev, Laser Phys. Lett. **7**, 677 (2010).
[23]J. Sancho-Parramon, V. Janicki, and H. Zorc, Opt. Express **18**, 26915 (2010).
[24]M. J. Weber, *Handbook of Optical Materials* (CRC, Florida, 2003).
[25]D. E. Aspnes and A. A. Studna, Phys. Rev. B **27**, 985 (1983).
[26]P. B. Johnson and R. W. Christy, Phys. Rev. B **6**, 4370 (1972).
[27]A. Hilger, M. Tenfelde, and U. Kreibig, Appl. Phys. B: Lasers Opt. **73**, 361 (2001).
[28]A. Pinchuk, U. Kreibig, and A. Hilger, Surf. Sci. **557**, 269 (2004).
[29]P. Yeh, *Optical Waves in Layered Media* (Wiley, Hoboken, NJ, 2005).

Author complimentary copy. Redistribution subject to AIP license or copyright, see http://apl.aip.org/apl/copyright.jsp